Evaluation of Microparticle Hydrogels in an *In Vivo* Subcutaneous Model

by

Brittany St. Martin

B.S., University of Colorado, 2019

A thesis submitted to the

Faculty of the Graduate School of the

University of Colorado in partial fulfillment

of the requirement for the degree of

Master of Science

Mechanical Engineering

2019

Signature Page

This thesis entitled:

Evaluation of Microparticle Hydrogels in an *In Vivo* Subcutaneous Model

written by Brittany St. Martin

has been approved for the Department of Mechanical Engineering

_____

Prof. Corey Neu

Date_____

_____

Prof. Alaa Ahmed

Date_____

The final copy of this thesis has been examined by the signatories, and we find that both the content and the form meet acceptable presentation standards of scholarly work in the above mentioned discipline.

IACUC protocol # 2628

Abstract

St. Martin, Brittany (M.S., Mechanical Engineering)

Evaluation of Microparticle Hydrogels in an *In Vivo* Subcutaneous Model

Thesis directed by Associate Professor Dr. Corey Neu

Hydrogel scaffolds are currently being explored as possible methods to aid in tissue regeneration and regrowth. Hyaluronic acid (HA)-based scaffolds are biocompatible and promote cell growth, but unfortunately, they also degrade rapidly (within weeks to months) following *in vivo* implantation in subcutaneous models, prior to substantial regrowth. To overcome challenges in implant longevity, we explored a possible tissue scaffold solution using HA crosslinked with polyethylene glycol diacrylate (PEGDA) hydrogels that were additionally augmented with decellularized microparticles of native tissue extracellular matrix. To study the *in vivo* response and compare between decellularized tissue types—skin, cartilage, adipose, and skeletal muscle—the hydrogels were implanted subcutaneously in a murine model for one and three months. We found that after both one and three months, the hydrogels containing decellularized particles persisted longer than HA/PEGDA alone (particle-free controls), with the exception of skin particles at one month. Of the surviving gels after one month *in vivo*, all hydrogels with decellularized tissue, except for skeletal muscle samples, had a larger volume retention percentage from the original volume than the control gels. After three months, adipose and cartilage tissue hydrogels had a larger volume retention than the controls. Additionally, it was found that the cellular infiltration distance into the hydrogel was higher for gels containing tissue particles compared to controls. We additionally observed minimal angiogenesis in all

hydrogel types, with comparatively more angiogenesis quantified in hydrogels augmented with skeletal muscle particles. These results demonstrate that the inclusion of decellularized tissue particles in HA/PEGDA hydrogels increases implant survival and recellularization, proving valuable in aiding tissue regeneration by acting as a long-lasting cellular scaffold for regrowth.

Acknowledgements

Firstly, I would like to acknowledge my advisor, Dr. Corey Neu for his guidance and expertise throughout this research. I would also like to thank my thesis committee—Dr. Alaa Ahmed, Dr. Wei Tan—for their support of my research and studies.

I am extremely grateful for the mentoring and support Jeanne Barthold gave me from when I first joined the lab until the end of my work. My research would not be possible without her significant contributions. I also want to thank Stephanie Ellyse Schneider, who provided assistance in experiments and endless advice. To my fellow lab members—Alexis Waquez, Adrienne Scott, Kaitlin McCreery, Bobby Wilson, Dr. Ben Seelbinder, and Dr. Soham Ghosh—thank you for your support of my research, in many ways.

I also want to show appreciation to Barb Bogner for always supporting me and providing both personal and professional opportunities to grow and learn. To my best friend, Sarah Larson, thank you for always being there for me. Finally, I want to thank my family for always being my number one supporter. Your endless love and support helped me in so many ways. I would not be the person I am today without you.

Scientific Acknowledgments

I appreciate the contribution to this research made by E. Erin Smith, Allison Quador and Jessica Arnold of the University of Colorado Denver Tissue Biobanking and Histology Shared Resource.

Contents

Table of Figures

Introduction

The extracellular matrix (ECM) is a complex physical scaffold made up of different molecules, such as proteins and glycosaminoglycans. It is found in all types of tissues and organs, providing physical and biochemical cues for cells[1]. These cues aid in guiding and regulating cellular differentiation and apoptosis, essential for successful tissue homeostasis and regeneration[2]. The ECM also provides a physical structure for cell attachment. The unique ability for tissue ECM to provide both mechanical and biochemical signaling had made decellularized ECM scaffolds a focus of tissue regeneration. An ideal scaffold for tissue regeneration will act as a substrate for cells to attach and proliferate on, provide tissue specific mechanical framework, and integrate into the existing native tissue. Current trends in research have tried to address these concerns when creating scaffolds.

Hydrogels, such as collagen, have become a popular solution for tissue regeneration because they can be developed to easily degrade *in vivo* while still providing a structure for cells to proliferate on. Additionally, many hydrogels, such as hyaluronic acid (HA), are composed of materials that naturally occur within the body[3]. However, the mechanical properties of hydrogels do not always match the tissue type that is being regrown, which can prevent successful regrowth. To more closely capture the ideal characteristics from the ECM, several techniques involve decellularizing tissue and using the decellularized tissue itself as a scaffold. Cook Biotech Inc. developed a decellularized small intestine submucosa sheets to aid in skin regeneration[4,5]. This provides a true ECM structure, including many biochemical molecules important in tissue regrowth. However, these sheets are often thin, limiting their application.

Other possible solutions for tissue regeneration scaffolds include decellularizing tissue microparticles and forming a composite hydrogel with the microparticles. One type of composite hydrogel was made from hyaluronic acid (HA) and polyethylene glycol diacrylate (PEGDA). HA exists naturally in multiple types of native tissue ECM and is known to be biocompatible[6]. The PEGDA is added to the hydrogel as a crosslinker to provide structure and stability to the hydrogel. *In vitro* cell work has been completed with these composite hydrogels specifically looking into articular cartilage regeneration[7–10]. While *in vitro* studies with this composite showed promising results, the system has not been tested *in vivo*. A commonly used initial *in vivo* study for tissue regeneration scaffolds is a subcutaneous model because it provides an easily executable study to look into biocompatibility, initial cell response, and scaffold degradation, before completing a complex tissue-specific *in vivo* model[11–13].

The goal of this project was to evaluate microparticle hydrogel implants in an *in vivo* subcutaneous environment. To achieve this goal, we first expanded and optimized established decellularization and scaffold formation techniques to multiple tissue types. Second, we designed, executed, and evaluated a murine *in vivo* study looking specifically at subcutaneous implants over multiple time periods.

Materials and Methods

Microparticle Decellularization

A decellularization process was developed and adapted for four different tissue types: adipose, cartilage, skeletal muscle, and skin. Tissue was first particulated using a Qiagen Tissue Lyser in combination with liquid nitrogen to grind the tissue from its native form into microparticles. Decellularization was found to be more effective when the tissue was in microparticle form, as any liquid used to decellularize could easily permeate fully into the tissue.

At 37 ℃ under agitation, the tissue was decellularized in 2% sodium dodecyl sulfate (SDS) to break apart cellular membranes, allowing for cellular materials to be removed from the tissue. The microparticles were then rinsed in 1X PBS to remove remaining SDS detergent along with any excess cellular material. The tissue was then further decellularized with a 0.1% DNAse wash to degrade remaining DNA fragments into non-functional, smaller pieces. To sterilize the decellularized microparticles, they underwent a 30-minute 70% ethanol rinse, followed by a 30-minute sterile 1X PBS rinse. It can be noted that all procedures during decellularization were done with sterile technique, including sterile materials, tools, and in a biosafety cabinet. Finally, the tissue was lyophilized for 24 hours and stored in -80℃.

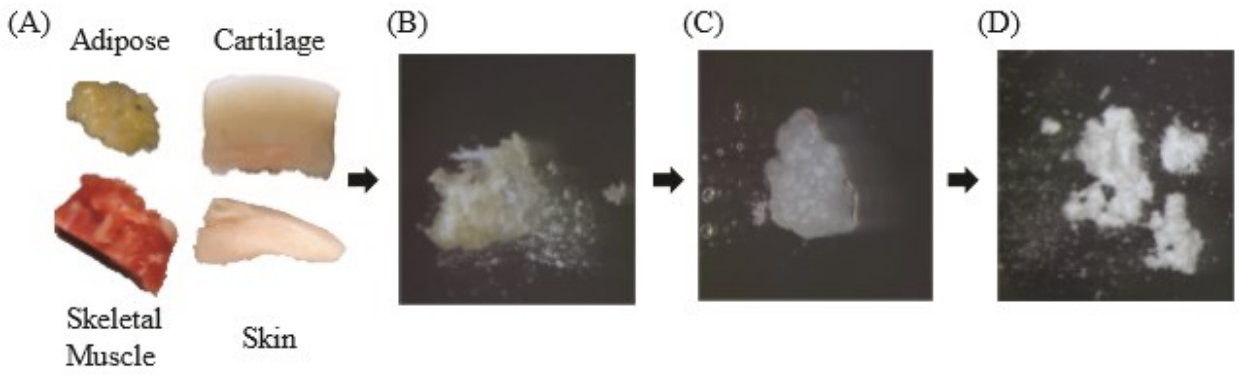

Figure 1: Multi-tissue decellularization process. (A) Native tissue is particulated into (B) tissue microparticles using a tissue lyser, then (C) decellularized in 2% SDS and 0.1% DNAse and then (D) sterilized with 70% ethanol and lyophilized, forming a fine powder.

The SDS detergent wash, 1X PBS rinse, and 0.1% DNAse wash steps were optimized for each tissue type, resulting in differing times for those three steps, which are detailed below for each specific tissue type.

Adipose Tissue

Adipose tissue was obtained from human donors through liposuction procedures, particularly from donor's abdomen resulting in white adipose tissue. The tissue was freshly harvested, briefly rinsed in 1X phosphate buffer saline (1X PBS) to remove excess blood and burnt tissue sections were manually removed. It was then flash frozen and stored in -80℃ until processed. The tissue was particulated as described above. Prior to the decellularization process, the microparticles were rinsed with 1X PBS and centrifuged at 3000 RPM for 5 minutes to separate and remove lipids. The decellularization process then continued, with the SDS detergent wash being for 24 hours, 1X PBS rinse for 12 hours, and 0.1% DNAse for 6 hours.

Articular Cartilage Tissue

Articular cartilage tissue was obtained from market weight porcine tissue, within 48 hours of animal slaughter and stored in -80℃ until processed. The decellularization process was as described above, with an 8-hour SDS detergent wash, 6-hour 1X PBS rinse, and 3 hours of 0.1% DNAse.

Skeletal Muscle Tissue

Skeletal muscle tissue was obtained from market weight porcine tissue, within 48 hours of animal slaughter and stored in -80℃ until processed. The decellularization process followed the same time points for the SDS detergent wash, 1X PBS rinse, and 0.1% DNAse wash steps as adipose tissue (24 hours, 12 hours, 6hrs respectively).

Skin Tissue

Skin tissue was obtained from market weight porcine tissue, within 48 hours of animal slaughter. Once obtained, excess adipose tissue on the skin was manually removed and then it was stored in -80℃ until processed. The decellularization process was completed as described

above for the adipose tissue, with the only exception being the SDS detergent wash was for 8 hours.

DNA Extraction and Isolation

Using a Sigma Aldrich Mammalian Genomic DNA Miniprep kit and specified protocol, the DNA from both native and decellularized tissue samples were extracted and isolated. Briefly, the tissue was digested and then the cells were lysed from the sample. After several washes, the DNA was then eluted into a final solution. The ng/μL of DNA in the samples was calculated using a Thermo Scientific NanoDrop. The DNA amount was normalized with the initial weight of the sample, resulting in the ng of DNA per mg of tissue.

DAPI Staining and Confocal Imaging

Samples of both native and decellularized tissue were stained with DAPI in 1X PBS at a concentration of 5μL/mL for 5 minutes, followed by 3 rinses in 1X PBS. The samples were then imaged on an inverted Nikon confocal microscope using a 405 nm laser, with both 10X and 20X objectives.

Microparticle Hydrogel Formation

Microparticle hydrogels consist of two components: decellularized microparticles and HA/PEGDA hydrogel. The hydrogel consists of crosslinked hyaluronic acid (HA) and polyethylene glycol diacrylate (PEGDA). First, thiolated HA (25-32% thiolated) is lyophilized and dissolved in 1X PBS. PEGDA, also dissolved in 1X PBS is combined with the aqueous HA solution, resulting in mixing of the HA thiol groups and PEGDA diacrylate groups at a ratio of 1:0.8 thiols:diacrylate. The combined viscous solutions are placed at 37℃ for 30 minutes, where Michael-type addition crosslinking occurs, resulting in a stable 3D hydrogel[14].

Prior to placing the solutions in 37℃, the microparticles must be added. The lyophilized, decellularized microparticles are first sorted, excluding all particles greater in size than 250 μm. Then, 8 mg of particles were evenly placed in a circular PDMS mold. The combined HA/PEGDA aqueous solution is added to the mold, filling the spaces between the particles. The resulting composite of densely packed microparticles in HA/PEGDA viscous gel is then placed at 37℃ for 30 minutes to allow crosslinking of the gel around the particles. The composition of these hydrogels are majority microparticles, with the HA/PEGDA hydrogel acting as a glue to hold the particles together. Microparticle hydrogels are stored in 1X PBS at 4℃ for 24 hours before implantation.

Each hydrogel, control or microparticle filled, was a cylinder that was 6 mm in diameter and 1.5 mm in height. An example of both types of hydrogels—with and without microparticles—is shown below in Figure 2, showing the highly packed microparticle density in the microparticle hydrogel.

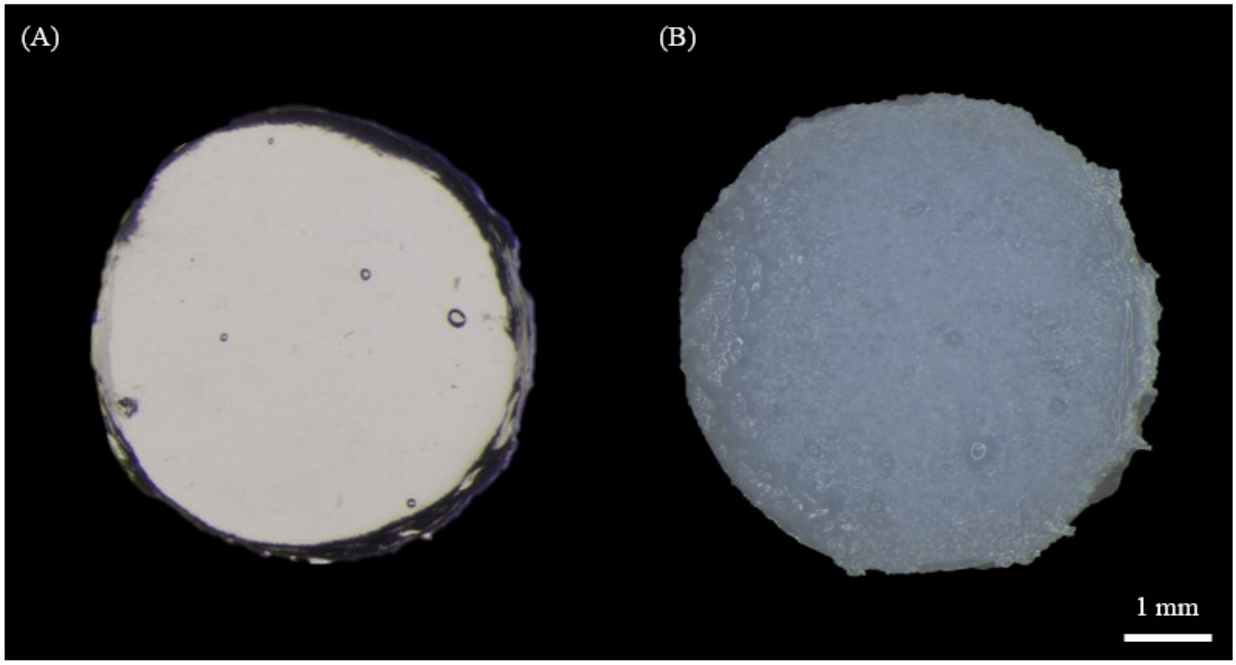

Figure 2: Example hydrogels for both (A) control and (B) microparticle hydrogels (Scale bar is 1 mm).

Endotoxin Testing

Before implanting any hydrogels in an animal, a sample hydrogel from each batch was tested for endotoxin levels using a Genscript Limulus Ambeocyte Lysate (LAL) gel clot endotoxin test kit, with a sensitivity of 0.25 Endotoxin Units/ml. Briefly, hydrogel samples were homogenized in LAL reagent water and then added to a LAL activated solution. The vials were incubated at 37℃ for one hour. After incubation, the vials were inverted to test for gel formation. Gel formation indicates a positive endotoxin result (>0.25 EU/ml). Each round of testing included a positive and negative control sample, and the test was repeated if either control was not as anticipated.

Mice

All animals used in this study were C57BL/6J male mice from Jackson Laboratories. Animals acclimated to their surroundings following shipping for one week. At time of surgery, the mice were 8 weeks old. All procedures were done in accordance to and approved by the Institutional Animal Care and Use Committee by the University of Colorado at Boulder.

Subcutaneous Implantation

Microparticle hydrogels were implanted subcutaneously in mice, using a process shown in Figure 3. The mice were first anesthetized using isoflurane. They were then tested for sensation by the pedal response. Following this, the animals were given 4 mg/kg of Meloxicam subcutaneously and were shaved in the surgical area. The surgical region was prepped with a betadine solution, followed by an additional response test. Two one-centimeter vertical incisions were made on their backs between either the shoulder blades or the hips. To the left and right of each incision, a subcutaneous pocket was made by blunt dissection, totaling in four pockets per animal. In each pocket, one hydrogel—either with or without microparticles—was implanted

(location randomized). The wounds were closed using wound clips, which were removed once the incisions healed (10-14 days post-op).

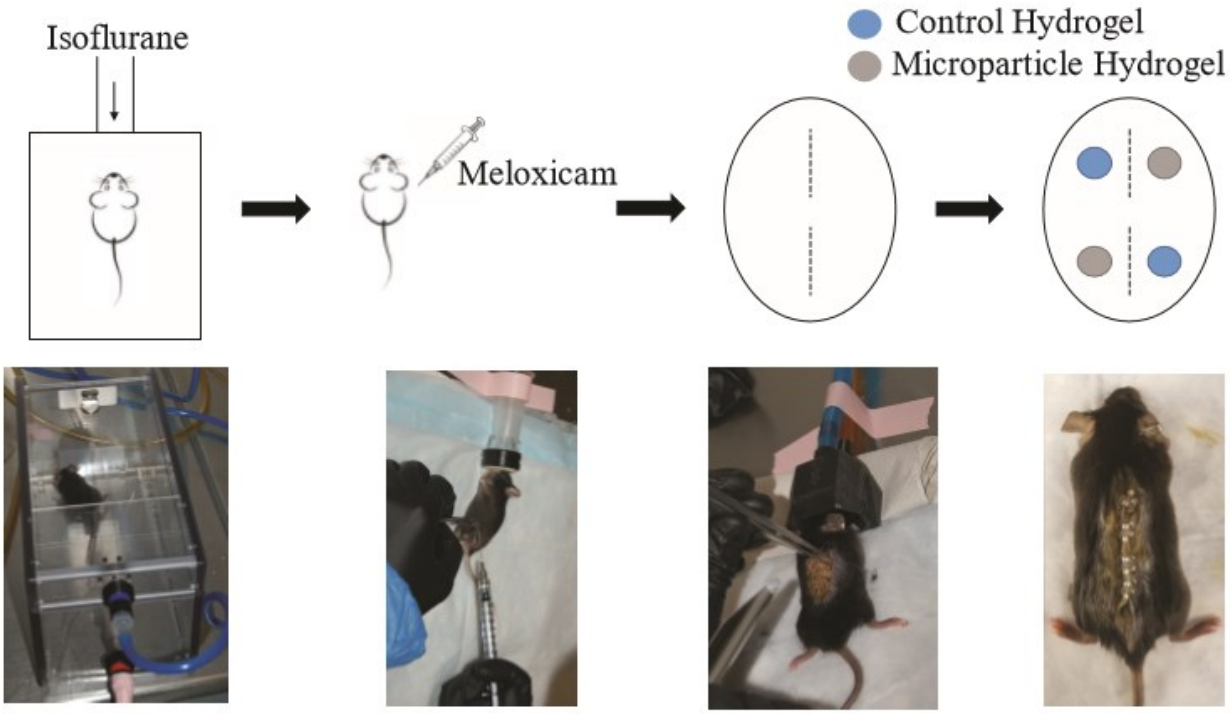

Figure 3: Subcutaneous Implantation Surgical Process. Animals are put under anesthesia and given a short-term subcutaneous analgesic. Two 1-centimeter long incisions are made on their back, depicted by the dotted lines, then 4 hydrogels are implanted per mouse, 1 on each side of each incision. Wounds are closed with wound clips and the animal is observed during recovery.

The subcutaneous implant study consisted of four treatment groups—the decellularized tissue microparticle hydrogels (adipose, cartilage, skeletal muscle, skin)—and one control group (HA/PEGDA hydrogel with no microparticles). Each mouse had two control gels and two microparticle hydrogels from the same treatment group, in randomized locations. For this study, two time points were chosen: 1 month and 3 months. These time points were chosen to allow for short-term and long-term evaluation of the hydrogels in an *in vivo* environment, based on previous literature[11,12,15–18]. For each time point, there were 12 hydrogels implanted per treatment group and 48 control hydrogels implanted.

Post-Surgical Observations

The animals were monitored daily for ten days following the surgery. They were monitored for incision healing, behavioral cues to indicate adverse reactions to either the surgery or the implants (e.g. cuddling, pinched face), and for implant inflammation. Implant inflammation was detected visually by looking for redness or swelling of the skin above and surrounding the implants.

For the duration of the study, the location of each implant was recorded twice a week. Additionally, the animals were weighed and monitored twice a week to record changes in weight post-op.

Hydrogel Dissection

After one or three months, the animals were sacrificed via CO_2 asphyxiation followed by cervical dislocation. The dissection process for each animal follows the process depicted in Figure 4. Immediately after sacrifice, the backs of each animal were shaved, implants and surrounding skin were dissected, and the dimensions of each implant were measured with calipers. Each explant was fixed in 4% paraformaldehyde (PFA) at 4°C for 48 hours before histological analysis.

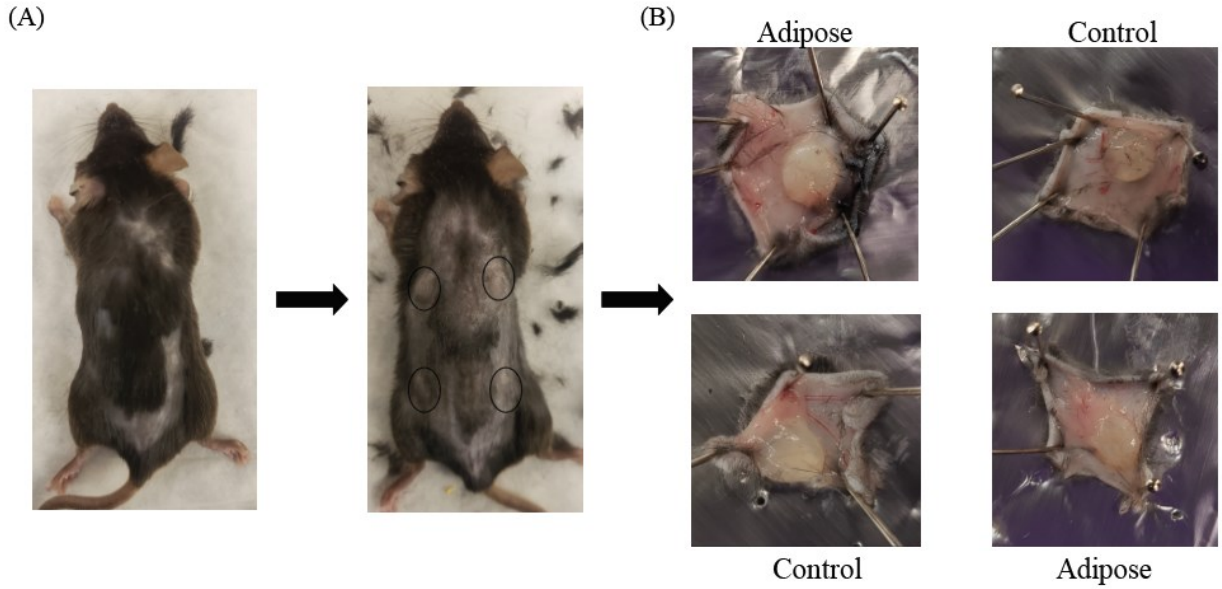

Figure 4: Hydrogel dissection procedure after 1 and 3 months. (A) Animals are euthanized, and their backs are shaved. The outlines of the four hydrogels are labeled by the circle on the back of the mouse. (B) The hydrogels and surrounding skin are dissected, with example images from an adipose 1-month group where 2 microparticle hydrogels and 2 control hydrogels were explanted.

Histological Preparation

Prior to dehydration and paraffin wax embedding, each hydrogel was cut in half. The hydrogels were then dehydrated and embedded in paraffin wax. 5 μm thick slices of the sample cross-sections were cut and mounted on histological slides for staining.

Masson's Trichrome Staining

All Masson's Trichrome staining was completed using a staining kit from Newcomer Supply. Samples were deparaffinized using SafeClear, then hydrated slowly through changes of ethanol, of decreasing concentrations, followed by a final hydration step of DI water. The tissues were then fixed in Bouin Fluid overnight at room temperature. Staining proceeded at room temperature as follows: Weigert Iron hematoxylin stain, Biebrich Scarlet-Acid Fuchsin stain, Phosphomolybdic-Phosphotungstic Acid wash, Aniline Blue stain, and Acetic Acid wash.

Finally, the samples were dehydrated in ethanol rinses, followed by rinses in SafeClear, and then a coverslip was mounted using Permount mounting medium.

This stain results in images composed of three colors: red, blue, and black. Red represents muscle fibers, cytoplasm, and keratin. Blue represents collagen and mucin. Black represents nuclei.

CD31 Staining

To complete the CD31 histological staining, the samples were deparaffinized in Xylene, then hydrate slowly through changes of ethanol, of decreasing concentrations, followed by a final hydration step in tap water. Antigen retrieval was completed using cell conditioning 1 (CC1). Using a Ventana Benchmark IHC stainer at 37℃, endogenous blocking was done followed by primary antibody staining (CD31 at 1:200 dilution). Next, mouse-rabbit polymer HRP was applied to the samples. DAB chromogen and copper enhancer was then applied to the samples, followed by Harris hematoxylin counterstaining. Samples were then dehydrated with increasing concentrations of ethanol, followed by clearing in Xylene. Finally, a coverslip was mounted using Cytoseal 60.

Histological Imaging

Images of both Masson's Trichrome and CD31 stained samples were taken using a Zeiss Brightfield non-inverted microscope at 5X, 10X, and 20X objectives. These images were then analyzed for various characteristics both quantitatively and qualitatively using the ImageJ particle analysis tool.

Statistical Analysis

A two-way ANOVA was used for all statistical analysis, with $p < 0.05$ considered significant. Error bars represent the standard deviation from the mean values.

Results

Tissue Decellularization

To confirm decellularization of the four tissue types, two commonly used methods of confirmation from literature were used: DAPI staining and DNA digestion/isolation[5]. Both native and decellularized tissue samples were stained with DAPI, as described in detail in the methods section. The images of the native and decellularized tissue samples were compared using particle analysis in ImageJ. The four tissue type images are below in Figure 5. In the figure, the native sample images for all four tissue types shows many nuclei, as expected for native tissue. Comparatively, the decellularized images show lack of nuclei, indicating the tissue was decellularized. It is important to note that there is autofluorescence occurring in the decellularized cartilage images, due to the distinct autofluorescence of tightly packed collagen fibers. This does not indicate a lack of decellularization however, as the blue signal is not showing distinct nuclei in the tissue.

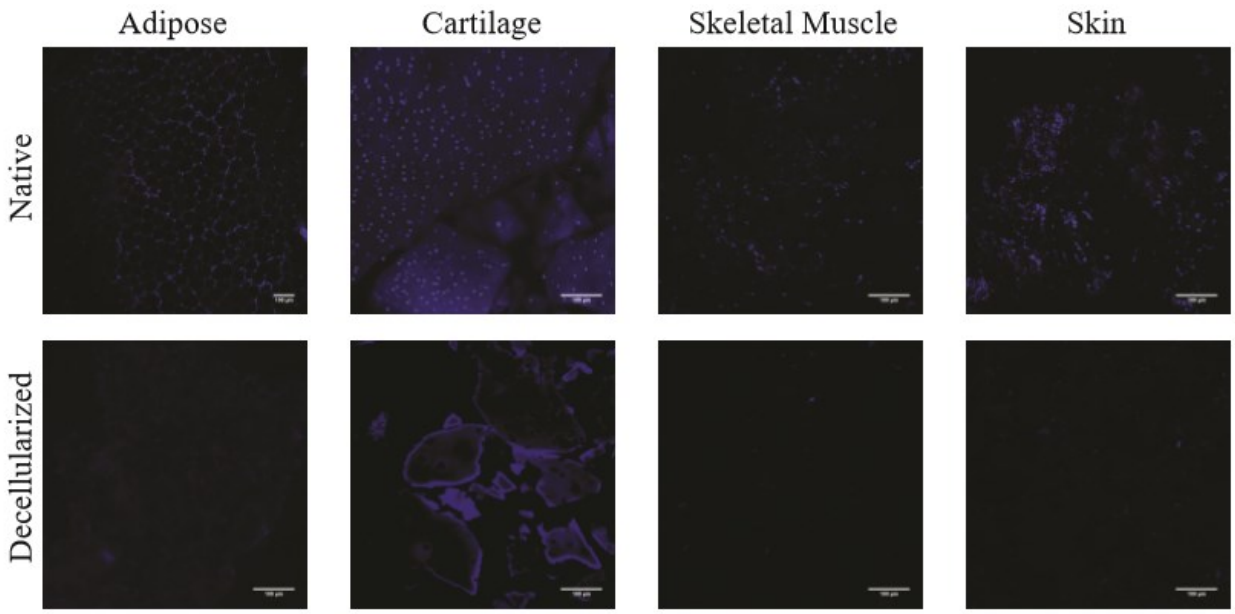

Figure 5: Native and decellularized DAPI stained images. The top row is native samples for the four tissue types (adipose, cartilage, skeletal muscle, and skin) and the bottom row is decellularized samples. The lack of nuclei in the decellularized images compared to native indicates successful decellularization (Scale bar is 100 μm).

The secondary method to confirm decellularization was DNA digestion and isolation. For all four tissue types, we measured the amount of remaining DNA—calculated as ng of DNA per mg of wet sample weight. The amount of DNA remaining in the decellularized sample was compared to its respective native DNA amount, resulting in a percentage of DNA remaining after decellularization compared to native tissue. The data is visualized below in Figure 6. In the figure, the native percentage is represented by the horizontal line at 100%. All four tissue types met our defined threshold by having less than 30% remaining DNA compared to native.

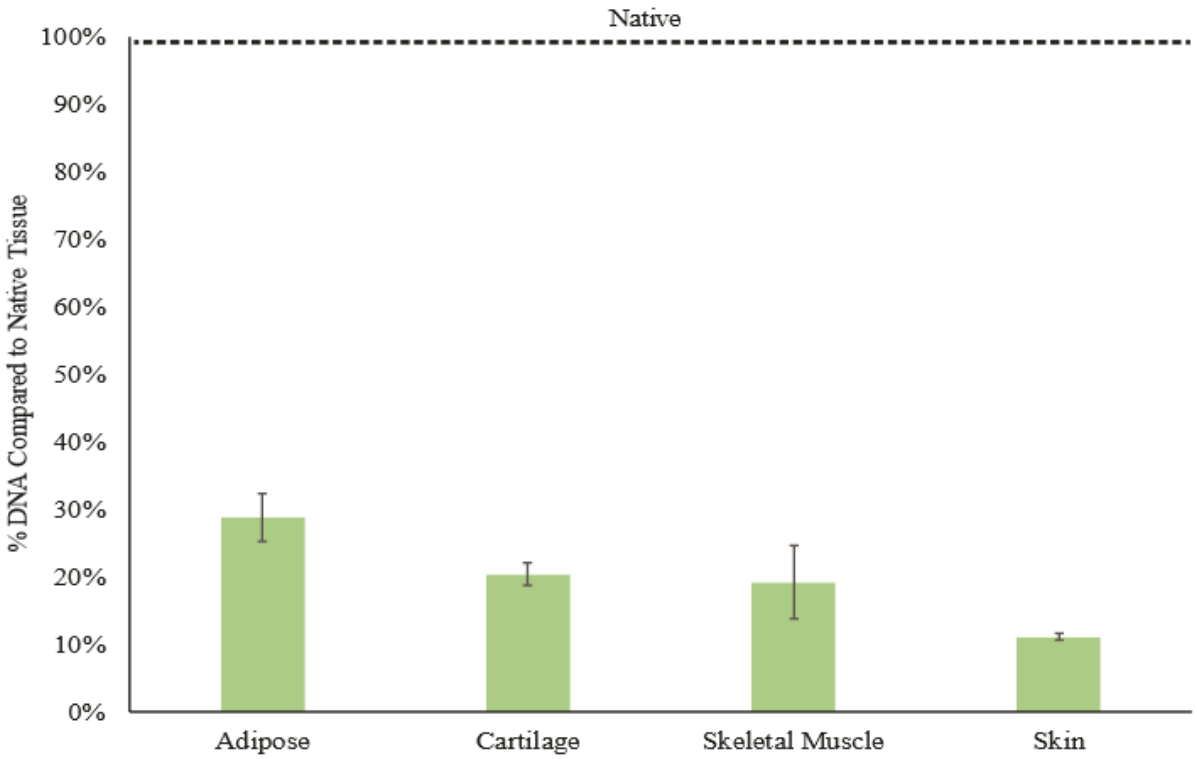

Figure 6: Remaining DNA percentages compared to native samples. Adipose, cartilage, skeletal muscle, and skin decellularized samples all had less than 30% remaining DNA when compared to their respective native samples, indicative of tissue decellularization.

Combining the results from the DAPI staining and the DNA digestion and isolation protocol, the four tissue types—adipose, cartilage, skeletal muscle, and skin—were concluded to be decellularized. While the DNA amount is not at zero percent, based on literature and in conjunction with imaging results, this conclusion was confidently made, and each batch was tested to meet these qualifications before endotoxin testing and implantation[5,19].

Post-Surgical Observations

Post implant surgery, we visually monitored the skin above each implant for redness and swelling as indicators of macroscale inflammation. At day 1 post-surgery, implants showed some signs of inflammation for all treatment groups and the control group, with the adipose microparticle hydrogels showing the highest percentage of inflammation. Throughout the next 10

days, the percentage of inflamed adipose hydrogels decreased. Comparatively, the control group initially had the lowest percentage inflamed, which also decreased over time (Figure 7). During the 10-day observation period, no treatment group had over 30% hydrogels inflamed. By day 5 post-surgery, all groups had 15% or less inflamed. At the time of sacrifice, either at 1 or 3 months, none of the hydrogels displayed visual signs of inflammation. With this data, we were able to conclude that any inflammation due to the implants decreased over time. With this decreasing inflammation over time, we concluded that no systematic inflammation occurred due to the implants, additionally shown by all animals staying healthy throughout the study.

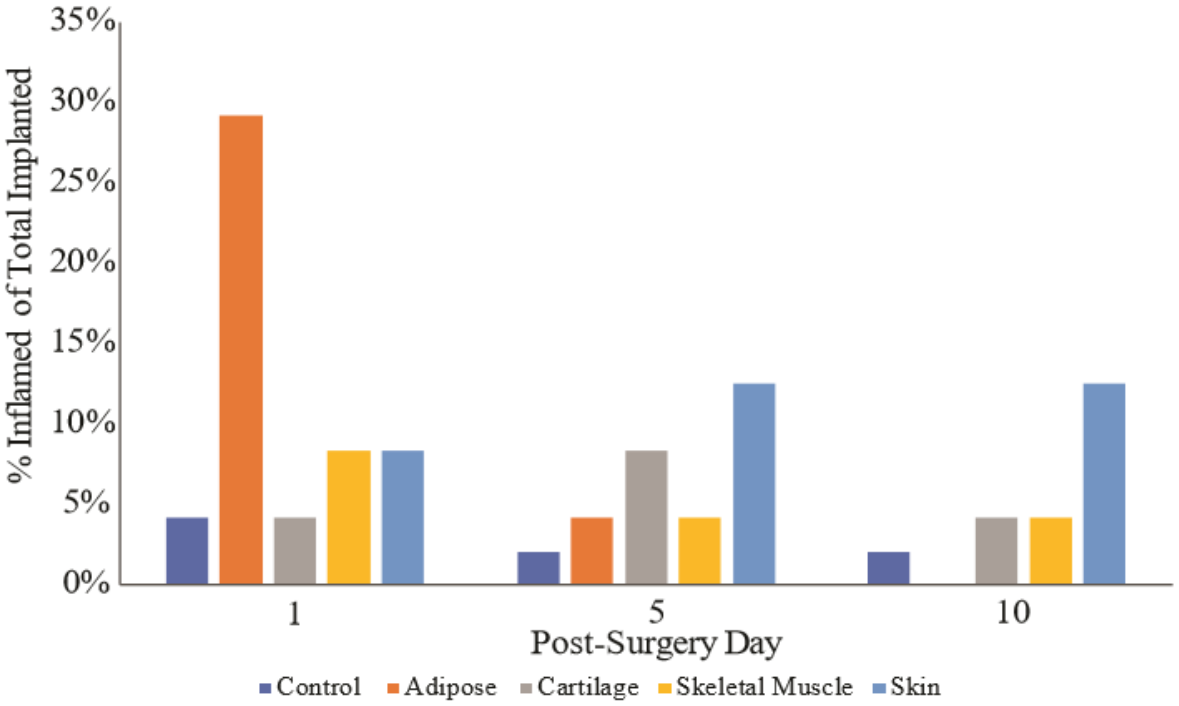

Figure 7: Hydrogel implant inflammation percentage post-surgery. Hydrogel implants were monitored for inflammation post-surgery, where inflammation for all types decreased over time, with no inflammation present at time of sacrifice (after 1 or 3 months).

An additional metric recorded throughout the study period included the weight changes in each mouse compared to their weight at time of surgery, as a way to monitor the overall health of

the animals and monitor systemic response to the implant. All mice gained weight over the study duration, following expected weight trends (Figure 8)[20]. A few mice lost weight immediately following surgery, possibly indicating short-term adverse reactions experienced from either the surgery or the implants. However, these mice gained the weight back quickly, and followed the same trends as the other mice throughout the remainder of the study, indicating no long-term adverse reactions to the implants. With both 1- and 3-month mice showing healthy weight trends, and no mice needing to be sacrificed early, it was concluded that no systematic adverse reactions occurred due to the hydrogel implants.

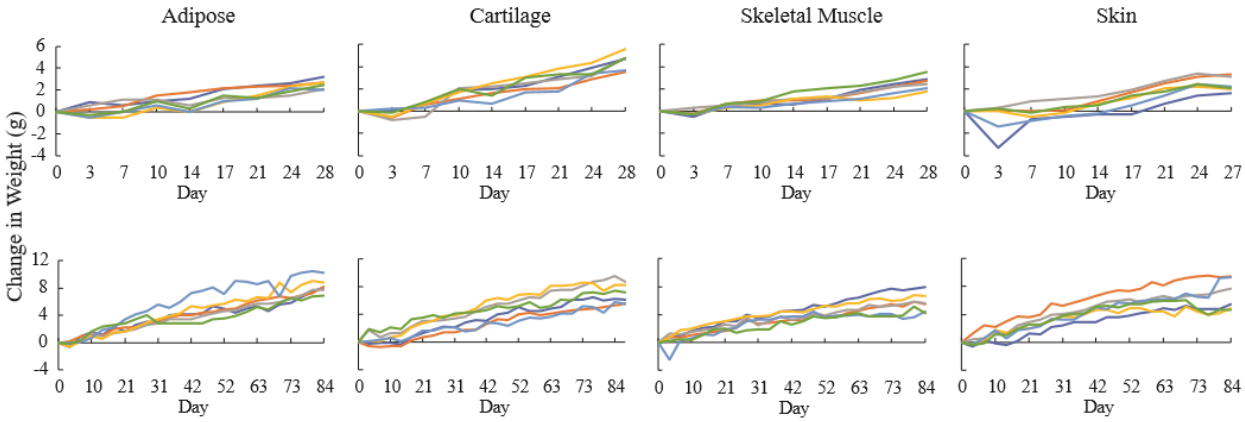

Figure 8: Animal weight changes post-surgery show healthy weight trends. Each animal's weight changes over study duration are represented by one line, grouped together by treatment group. The top row is the 1-month duration and the bottom row is the 3-month duration. All animals' weight changes compared to surgery day increased, proving that all animals remained healthy with no adverse reactions to the implants for the study duration.

Hydrogel Degradation

The hydrogel degradation *in vivo* was characterized by hydrogel persistence over time and by volume retention between implantation and explantation.

Hydrogel persistence varied between treatment groups, but overall persistence was higher in treatment groups than control hydrogels. Of the hydrogels for each type implanted, a percentage of hydrogels remained at the end of 1 or 3 months to be explanted, resulting in a

percentage hydrogel persistence for each group (Figure 9A). At the 1-month time point, cartilage, skeletal muscle, and adipose hydrogels had a 100% persistence percentage, which was greater than that of the control at 83% persistence. Between the 1-month and 3-month time points, all persistence percentages decreased, indicating a degradation of the hydrogels occurring over time. At the 3-month time point, all treatment groups—adipose, cartilage, skeletal muscle, and skin—had a higher percentage than the control percentage. Interestingly, adipose, skeletal muscle, and skin all had the same percentage at 3 months—75%--which, while lower than the cartilage percentage at 3 months, was still greater than control at 52%. Using a two-way ANOVA test, we found that both hydrogel type and implant duration was statistically significant, as demonstrated by the decrease in persistence from 1 to 3 months and the difference between the percentages for the microparticle hydrogels and the control hydrogels.

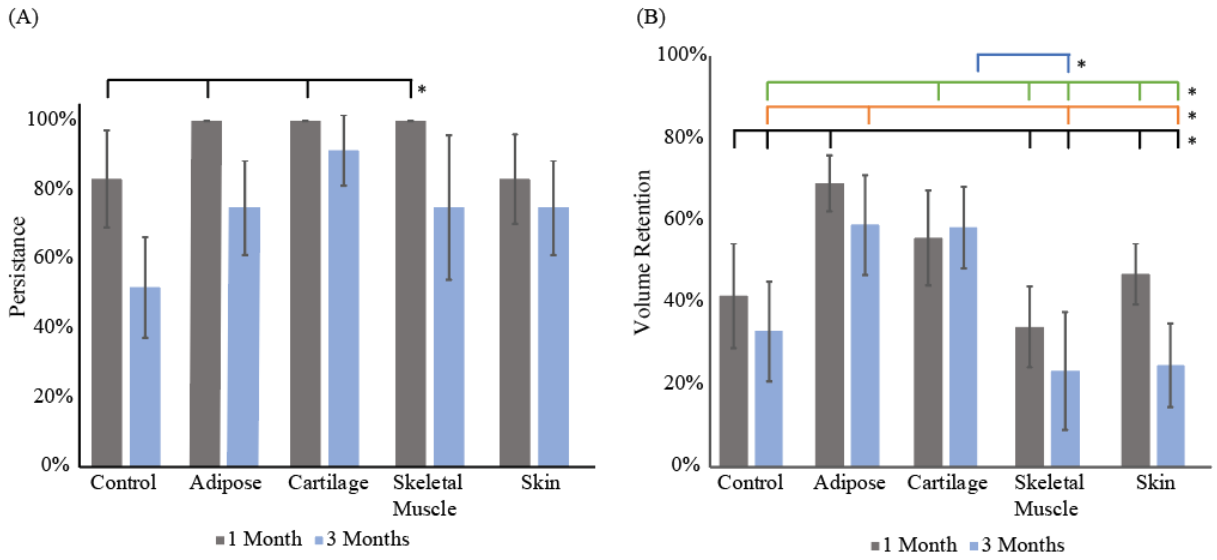

Figure 9: Hydrogel implant degradation defined by persistence and volume retention. (A) Hydrogel persistence over 1 and 3 months, with persistence decreasing over time for all hydrogel types. Microparticle hydrogels have higher persistence than control hydrogels. Both hydrogel type and implant duration are statistically significant for persistence. (B) Volume retention of persisted hydrogels between explantation and implantation, with volume retention generally decreasing over time. Both hydrogel type and implant duration are statistically significant for volume retention. (* $p < 0.05$).

To look at degradation amounts in more detail, we also calculated the volumes of the surviving hydrogels compared to the volume prior to implantation, (Figure 9B). Both implant type and duration were found to be significant covariates in determining the mean volume retention percentage. Particularly, both adipose and cartilage hydrogels were significantly different in mean volume retention percentage than the control, skeletal muscle, and skin hydrogels. Looking closer at the data, the volume retention percentage generally decreased over time, again indicating a steady degradation occurring over time, at different rates depending on the microparticle tissue type. These different rates are seen by the lower volume retention percentages for skin and skeletal muscle than cartilage and adipose. In the case of skeletal muscle, both 1- and 3-month time periods had lower retention than the control gels, indicating the skeletal muscle microparticles have a faster degradation rate—in terms of volume—than the control. Overall however, the presence of particles increases overall persistence and decreases degradation rate, as compared with control HA/PEGDA implants.

Hydrogel Visual Characteristics

Masson's Trichrome staining is useful to visualize characteristics of explants including cell infiltration, integration, and treatment group specific responses (Figure 10). At both 1 and 3 months, control HA/PEGDA hydrogels had a distinct fibrous, collagen capsule surrounding the hydrogel. Additionally, there was a lack of nuclei within the hydrogel, demonstrating no integration or strong cellular response from host tissue.

The first treatment group, adipose microparticle hydrogels, showed a similar fibrotic collagen capsule surrounding the implant. The fibrotic capsules surrounding the adipose hydrogels were thicker than in control hydrogels. However, we also find increased cellular infiltration from host tissue into the adipose hydrogels, although the cells still remain close to

outer edge of the implants, increasing only slightly between 1 and 3 months. Cartilage microparticle hydrogels have a distinct pattern because cartilage particles are distinguishable from the hydrogel portion. In cartilage explants, increased numbers of cells infiltrated into the hydrogel, and surrounded the tissue particles. From 1 to 3 months, the cell infiltration increases towards the center of the explant, showing a time dependent cellular response in this treatment group. Furthermore, the fibrotic capsule seen in controls, is much more integrated into the host tissue in cartilage explants, indicating a different kind of implant-host response. Skeletal muscle microparticle hydrogels showed a similar trend to cartilage in that we see a fibrous capsule region, but it is more integrated into the host tissue. At 1 and 3 months, skeletal muscle hydrogels had a high cellular infiltration rate starting from the outer edges of the hydrogel moving inward. This infiltration appears to be the highest at the edges of the implant—the edges perpendicular to the skin layer. The final treatment group is the skin microparticle hydrogels. Skin microparticle hydrogels did not have an easily visible capsule that surrounded the hydrogel, indicating improved integration with host tissue. Skin microparticle hydrogels have high cellular infiltration that unlike other tissues decreases from 1 to 3 months, demonstrating a potentially different type of host response than seen in other treatment groups.

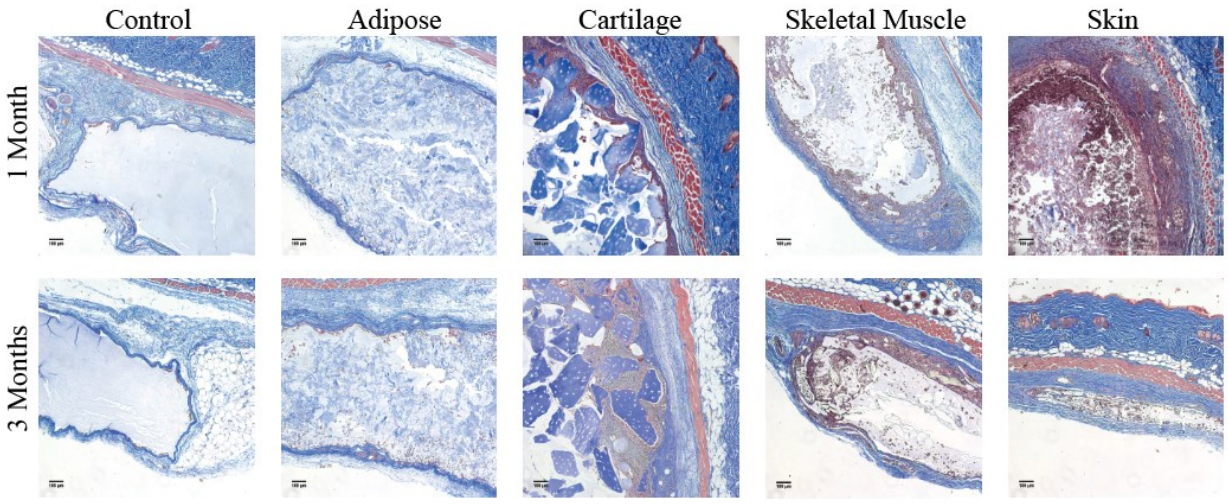

Figure 10: Masson's Trichrome staining of the different hydrogel types. For all hydrogel types (4 treatment groups, 1 control), representative figures for both 1 and 3-months are included. These images highlight differences in cellular infiltration, capsule presence, and host reaction. For reference, the top right corner of the control 1-month image is the dermal layer, with the epidermis above it. (Extended anatomical references in the Appendix, scale bar is 100 μm).

Cellular Infiltration

Implant success is partially driven by high cell infiltration into the implant, as the cells can then regrow and replace damaged tissue. Using the outer edge of the capsule as a reference point, the distance that cells traveled into the implants was measured and then normalized against the implant radius (Figure 11A). Skin and skeletal muscle infiltration percentages were found to be statistically different using a two-way ANOVA from those of adipose, cartilage, and control hydrogels, with both 1-month and 3-month skin and skeletal muscle infiltration percentage means being larger than the other types (Figure 11B). However, skin and skeletal muscle also have larger degradation rates, seen by their volume retention percentages between 1 and 3 months, so there may be a correlation between cellular infiltration and degradation.

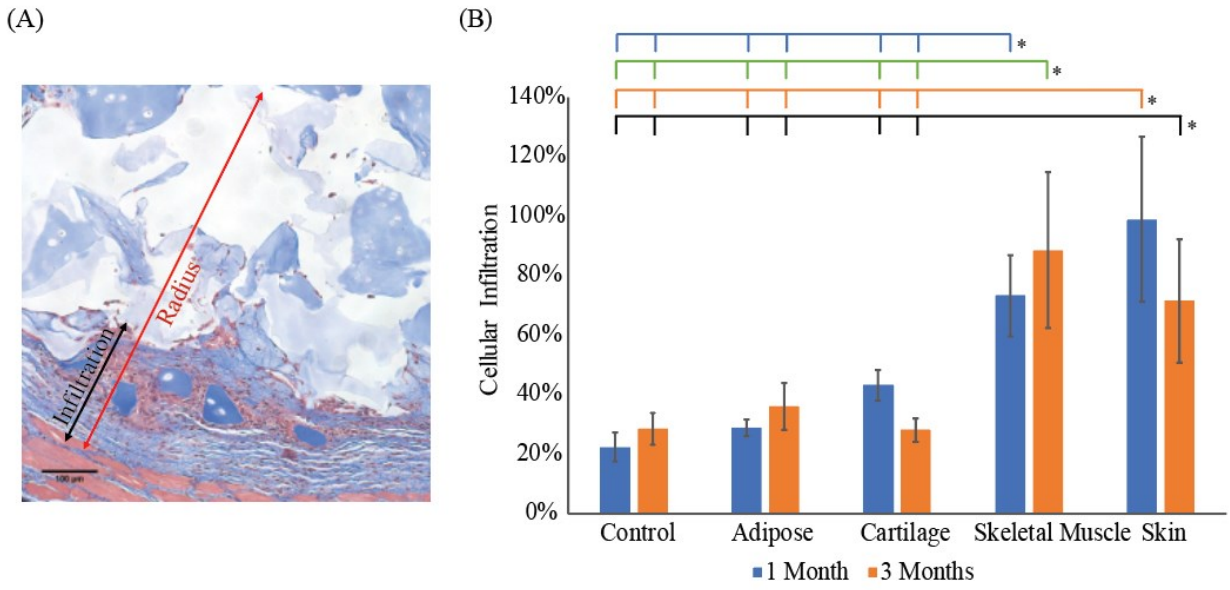

Figure 11: Cellular infiltration into hydrogel implants. (A) Infiltration was measured from the outside border of the capsule inwards following continuous cell growth (black arrow). It was normalized by the hydrogel radius (red line). (B) Cellular infiltration percentages for all hydrogel types, where skeletal muscle and skin microparticle hydrogels have the highest infiltration. Hydrogel type was found to be statistically significant. (Scale bar is 100 μm. * $p < 0.05$).

Angiogenesis

To study angiogenesis, or blood vessel formation, in the hydrogel explants, samples were stained with a specific angiogenesis marker: CD31 (Figure 12A)[21]. Using the outside edge of the capsule surrounding the gels as a distinct outer perimeter of the gel, the area that was stained as positive for endothelial cell adhesion molecules—indicative of angiogenesis—out of the total gel area was calculated, resulting in a percentage area positive for CD31 (Figure 12B). Based on a two-way ANOVA, the implant type—control, adipose, cartilage, skeletal muscle, skin—was significant in determining the mean of percent area, with skeletal muscle being significantly different than adipose, cartilage, and control. The duration that the implant was *in vivo* was not found to be statistically significant in improving angiogenesis.

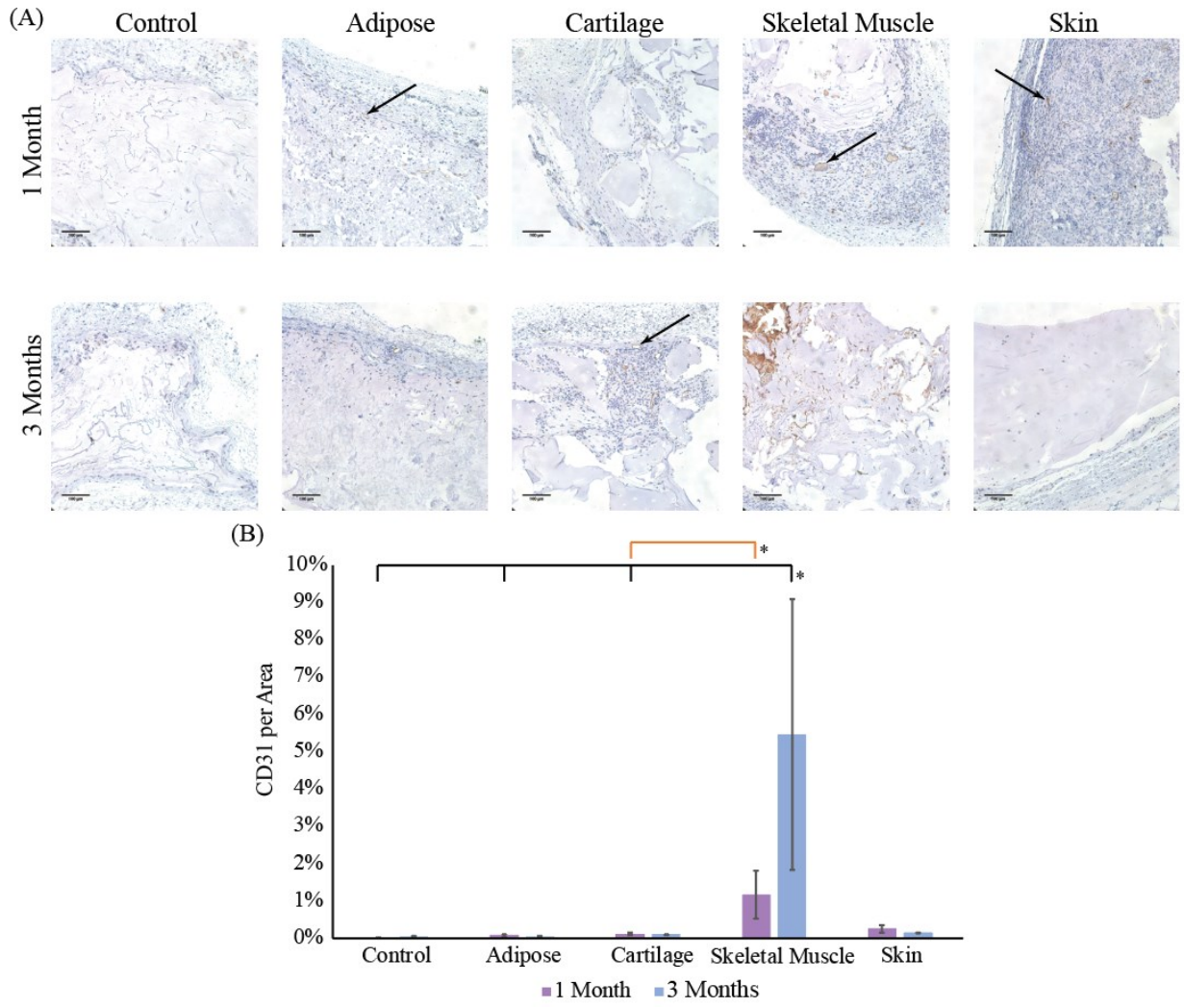

Figure 12: Minimal angiogenesis occurred within all hydrogel types. (A) Representative CD31 staining images for all hydrogel types for 1 and 3-month time points. The black arrows indicate examples of positive CD31 staining. (B) The percentage of positive CD31 staining per area for all hydrogel types shows less than 10% angiogenesis. Hydrogel type was found to be statistically significant. (Scale bar is 100 µm. * $p < 0.05$).

While skeletal muscle showed the highest significance for angiogenesis, all values fell below 10%. Skeletal muscle had the largest percentages; however, it also had the largest standard deviations, warranting further exploration. It can be comparatively noted that the area percentage for control 1-month samples is close to zero, indicating very little angiogenesis occurring.

Discussion

Based on the post-surgical observations, we found that all hydrogel types did not induce a systematic immune response from the animal. While we observed some early inflammation, it decreased over time. The immediate inflammation may be due to any remaining cellular material in the decellularized particles. For example, the adipose microparticle hydrogels had the highest initial percentage of inflammation and the adipose microparticles were the least decellularized of all the tissue types. Another possible reason for this increased inflammation in the adipose hydrogels is that the tissue was sourced from human, not porcine like the other tissue types. It is likely that continued optimization of the decellularization process could decrease this inflammation; however, it is not vital because there was no systematic reaction to any implant type that affected any animal's overall health. All animals were found to be healthy for the entire study duration. Decreasing the inflammation may aid in increasing the longevity of the hydrogel in the body, but further investigation is necessary.

All implanted hydrogels degraded over time, however cartilage hydrogels degraded the least over time, confirmed by both persistence percentage and volume retention. This may be due to the tightly woven natural ECM of cartilage, compared to the looser, more flexible ECM structure of the other tissue types. Slower degradation in cartilage hydrogels could also be attributed to the mechanical properties of the particles, which are stiffer than the other particle types. Degradation rates of microparticle hydrogel implants are important for tissue regeneration. If a scaffold degrades too quickly, no new tissue will be able to form. If it degrades too slowly, there will be no room for new tissue to form, and integration into native tissue will be limited. However, the importance of degradation rate is largely application dependent. For

example, a slow degradation rate may be important where there needs to be a constant mechanical support framework while new tissue is formed for functional reasons.

Additionally, in the realm of tissue regeneration, it is important to consider cellular infiltration into the implants, as new tissue cannot be regrown if there are no cells to create and maintain newly synthesized ECM. While cartilage hydrogels showed the least degradation over time, they did not show significant cellular infiltration, compared with skeletal muscle and skin. This example for our study demonstrates that there must be a balance between degradation and cellular infiltration to create the ideal tissue regeneration implant. It is also important to note that the hydrogel types that had the highest cellular infiltration also showed the most degradation This pattern is logical as the cells will aid in degrading the implant. Clearly, a balance between degradation and cellularity of the implant must be understood and optimized for success in specific applications. Another important observation to consider when looking at cellular infiltration is that skin microparticle hydrogels had a high percentage of infiltration, and unlike other tissues, it lacked a capsule surrounding the implant. Therefore, the fibrous capsule could inhibit cellular infiltration, as it is more difficult for cells to travel through the dense collagen fibers.

A critical component that this study was missing is to consider the cell type that infiltrates the microparticle hydrogels. There were different host responses to each tissue type, such as the high level of infiltration into the skin hydrogels at 1 month. We hypothesize that this is a macrophage response reacting to the implanted foreign body. The macrophages later leave the implant, possibly explaining the decrease in cellular infiltration noted between 1 and 3 months in the skin microparticle hydrogels. However, further investigation is needed to identify the cell types within and immediately surrounding the hydrogels. These future studies may lead

to more information about why certain tissue types were more infiltrated. It may also help identify if there is a correlation between cell type and degradation rates of the hydrogels.

A further evaluation of hydrogel implants is looking into new blood vessel growth which is vital for any tissue growth to be sustainable. There was minimal angiogenesis occurring in all hydrogel types for both 1 and 3 months. However, it is possible that the time points chosen are not long enough for angiogenesis to fully occur. Additionally, certain applications such as cartilage regeneration may not require as much blood vessel growth due to the avascular nature of native tissue.

Conclusion

This study evaluated the *in vivo* response of multiple types of decellularized microparticle hydrogels. Future work is necessary to further investigate tissue and cell specific responses *in vivo*. This includes identifying cell type, further define the localized foreign body reaction by looking at macrophages and identify any cell differentiation that may be occurring in specific hydrogel types.

Further *in* vivo work could also be completed for tissue specific applications of these microparticle hydrogels. For example, the skeletal muscle microparticle hydrogels could be applied to a volumetric muscle loss model. To further study these hydrogels, extended immunostaining and RT-qPCR should be completed for each tissue type. Additionally, it was recently found that specific growth factors can promote specific tissue growth. Previous studies have shown that TGF-β was preserved in the decellularized cartilage particles through the decellularization process, which is known to be involved in differentiation and ECM production in cartilage repair[10,22]. We hypothesize that similar growth factors are preserved in the other

decellularized tissue particles. Further investigation is required to confirm this hypothesis and relate growth factors to the *in vivo* responses seen in this study. Studying the growth factors present in the hydrogels while in their tissue-specific *in vivo* environment can aid in further development of ideal hydrogels for tissue regeneration.

This study has shown that the addition of decellularized tissue microparticles to hydrogels increases the longevity of the hydrogel *in vivo* by slowing degradation. It has also shown that these microparticle hydrogels have increased cellular infiltration over hydrogels without microparticles. Additionally, there is not systematic adverse reaction over time *in vivo* to the microparticle hydrogels. Further studies of these microparticle hydrogels will define localized inflammation responses, the role of growth factors conserved in the decellularized tissue, and the specific cellular response to each implant type.

Bibliography

1. Badylak, S. F., Freytes, D. O. & Gilbert, T. W. Extracellular matrix as a biological scaffold material: Structure and function. *Acta Biomater.* **5**, 1–13 (2009).

2. Beachley, V. *et al.* Extracellular matrix particle-glycosaminoglycan composite hydrogels for regenerative medicine applications. *J. Biomed. Mater. Res. Part A* **106**, 147–159 (2018).

3. Drury, J. L. & Mooney, D. J. Hydrogels for tissue engineering: scaffold design variables and applications. *Biomaterials* **24**, 4337–4351 (2003).

4. Cook Biotech. A World Leader in Regenerative Medicine - Technology | Cook Medical. Available at: https://www.cookbiotech.com/technology/. (Accessed: 3rd August 2019)

5. Crapo, P. M., Gilbert, T. W. & Badylak, S. F. An overview of tissue and whole organ decellularization processes. (2011). doi:10.1016/j.biomaterials.2011.01.057

6. Burdick, J. A. & Prestwich, G. D. Hyaluronic Acid Hydrogels for Biomedical Applications. *Adv. Mater.* **23**, H41–H56 (2011).

7. Novak, T. *et al.* In Vivo Cellular Infiltration and Remodeling in a Decellularized Ovine Osteochondral Allograft. doi:10.1089/ten.tea.2016.0149

8. Novak, T. *et al.* Dissociated and Reconstituted Cartilage Microparticles in Densified Collagen Induce Local hMSC Differentiation HHS Public Access Author manuscript. *Adv Funct Mater* **26**, 5427–5436 (2016).

9. Novak, T. *et al.* Mechanisms and Microenvironment Investigation of Cellularized High Density Gradient Collagen Matrices via Densification HHS Public Access. *Adv Funct Mater* **26**, 2617–2628 (2016).

10. Barthold, J. *et al.* Mechanically tunable dECM scaffold with tissue specific signaling that promotes cell migration, homing, and matrix deposition both in-vitro and in-vivo. (2019). (submitted)

11. Zhang, L. *et al.* Zwitterionic hydrogels implanted in mice resist the foreign-body reaction. *Nat. Biotechnol.* **31**, 553–556 (2013).

12. Modulevsky, D. J., Cuerrier, C. M. & Pelling, A. E. Biocompatibility of Subcutaneously Implanted Plant-Derived Cellulose Biomaterials. (2016). doi:10.1371/journal.pone.0157894

13. Azab, A. K. *et al.* Biocompatibility evaluation of crosslinked chitosan hydrogels after subcutaneous and intraperitoneal implantation in the rat. *J. Biomed. Mater. Res. Part A* **83A**, 414–422 (2007).

14. Nair, D. P. *et al.* The Thiol-Michael Addition Click Reaction: A Powerful and Widely Used Tool in Materials Chemistry. (2013). doi:10.1021/cm402180t

15. Zhang, D., Tan, Q.-W., Luo, J.-C. & Lv, Q. Evaluating the angiogenic potential of a novel temperature-sensitive gel scaffold derived from porcine skeletal muscle tissue. (2018).

doi:10.1088/1748-605X/aac275

16. Alberti, K. A. & Xu, Q. Biocompatibility and degradation of tendon-derived scaffolds. doi:10.1093/rb/rbv023

17. Jansen, L. E. *et al.* Zwitterionic PEG-PC Hydrogels Modulate the Foreign Body Response in a Modulus-Dependent Manner. (2018). doi:10.1021/acs.biomac.8b00444

18. Wang, L., Johnson, J. A., Chang, D. W. & Zhang, Q. Decellularized musculofascial extracellular matrix for tissue engineering. *Biomaterials* **34**, 2641–2654 (2013).

19. Gilbert, T. W., Freund, J. M. & Badylak, S. F. Quantification of DNA in Biologic Scaffold Materials. *J. Surg. Res.* **152**, 135–139 (2009).

20. The Jackson Laboratory. Body Weight Information for C57BL/6J (000664). Available at: https://www.jax.org/jax-mice-and-services/strain-data-sheet-pages/body-weight-chart-000664#. (Accessed: 3rd August 2019)

21. Delisser, H. M. *et al. Involvement of Endothelial PECAM-1/CD31 in Angiogenesis*. *American Journal of Pathology* **151**, (1997).

22. Qu, F., Guilak, F. & Mauck, R. L. Cell migration: implications for repair and regeneration in joint disease. *Nat. Rev. Rheumatol.* **15**, 167–179 (2019).

Appendix

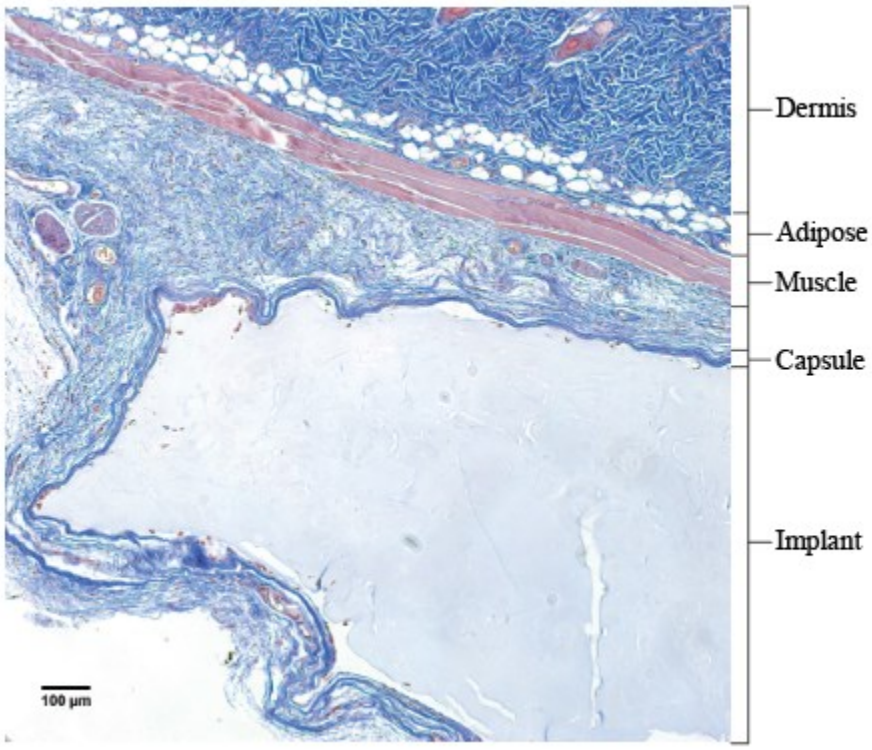

Figure A1: Anatomical references are labeled for a control 1-month sample. Starting at the top right corner is the dermis layer—above it would be the epidermis—and continuing downward is next an adipose layer, followed by a muscle layer. The next area is the subcutaneous pocket region where the hydrogel was originally implanted. Immediately surrounding the hydrogel is a collection of darker blue collagen fibers, called the capsule. Finally, the hydrogel implant is next when moving downward. (Scale bar is 100 µm).